RISKS OF PRE-MONSOON EXTREME RAINFALL EVENTS OF BANGLADESH: IS ANTHROPOGENIC CLIMATE CHANGE PLAYING A ROLE?

Ruksana H. Rimi, Karsten Haustein, Emily J. Barbour, and Myles R. Allen

Anthropogenic climate change doubled the likelihood of the 2017 pre-monsoon extreme 6-day rainfall event at northeast Bangladesh. The magnitude of this contribution is sensitive to the climatological period in use.

INTRODUCTION. Northeastern Bangladesh (NEB; 90.5°–92.5°E, 24°–25.5°N) has unique lowland areas known as *haors*. The "Boro" paddy (rice) crop is cultivated in these haors in dry winter season (December–February) and harvested during April–May. Boro accounted for ~55% of national rice production per annum during 2011–16 and NEB contributed to ~15% of the total Boro rice production over this period (FAO 2017). NEB receives highest annual mean rainfall of >4,300 mm, in contrast to western Bangladesh, which receives 1,400 mm (Shahid 2010). Topographic uplifting of the southwesterly flow by the Meghalaya Plateau and other surrounding mountains triggers heavy convective rainfall at NEB in the pre-monsoon season (Murata et al. 2008, 2011; Sanderson and Ahmed 1979; Shahid 2010). Pre-monsoon rainfall during March–April facilitates growth of Boro but events >150 mm of total 6-day rainfall can cause early flash floods and damage crops. On 27 March 2017, extreme rainfall over NEB triggered the earliest flash flood since 2000 (Ahmed et al. 2017). Subsequently, ~850,000 households were affected and ~220,000 ha of nearly harvestable Boro were damaged. Crop failure in 2017 contributed to a record 30% rice price hike compared to 2016 (FAO 2017). Analyzing NOAA's Climate Prediction Center (CPC) observation data, we find that during 16 March–15 April 2017, 6-day total rainfall over NEB amounted to 225 mm (i.e., 33.33% higher than the flash flood triggering threshold of 150 mm). The highest positive rainfall anomaly (up to 100 mm day^{-1}; relative to 1979–2017) during 16 March–15 April 2017 is found at NEB (see red box in Fig. 1a). To determine how rare this event is, we apply a generalized Pareto (GP) distribution fit to CPC data exceeding 90th percentile values, and find a return time of ~70 years (Fig. 1d).

Most of the attribution studies are done for midlatitude extreme events of the developed countries while very few of them focus on the tropical region (Marthews et al. 2015; Otto et al. 2015; Otto 2017) or developing countries, even though these countries experience extreme events and have the least capacity to adapt with the consequent impacts (IPCC 2013).

To understand the drivers behind the 2017 floods, here we investigate the probabilities of extreme 6-day rainfall during pre-monsoon season in Bangladesh and analyze whether or not anthropogenic climate change has changed the odds of such events occurring (Allen 1999). We utilize the very large weather@home regional climate model (RCM) ensemble based on HadRM3P. We also investigate the potential contribution of radiative cooling from anthropogenic aerosols as their presence can counterbalance the greenhouse gas (GHG) induced intensification of the hydrological cycle (Li et al. 2016). Niño-3.4 and Indian Ocean dipole (IOD) indices are used to quantify the role of two key climate modes. Additionally, two global climate models (GCMs) of MIROC5 and ETH_CAM4 are used to test the robustness of our results.

DATA AND METHODS. We use daily rainfall data from Asian Precipitation Highly Resolved Observational Data Integration toward Evaluation of Water Resources (APHRODITE) covering 1979–2007

AFFILIATIONS: Rimi, Haustein, and Allen—Environmental Change Institute, School of Geography and the Environment, University of Oxford, Oxford, United Kingdom; Barbour—Environmental Change Institute, School of Geography and the Environment, University of Oxford, Oxford, United Kingdom, and CSIRO Land and Water, Canberra, ACT 2601, Australia.
CORRESPONDING AUTHOR: Ruksana H. Rimi, ruksana.rimi@ouce.ox.ac.uk

DOI:10.1175/BAMS-D-18-0152.1

A supplement to this article is available online (10.1175/BAMS-D-18-0152.2)

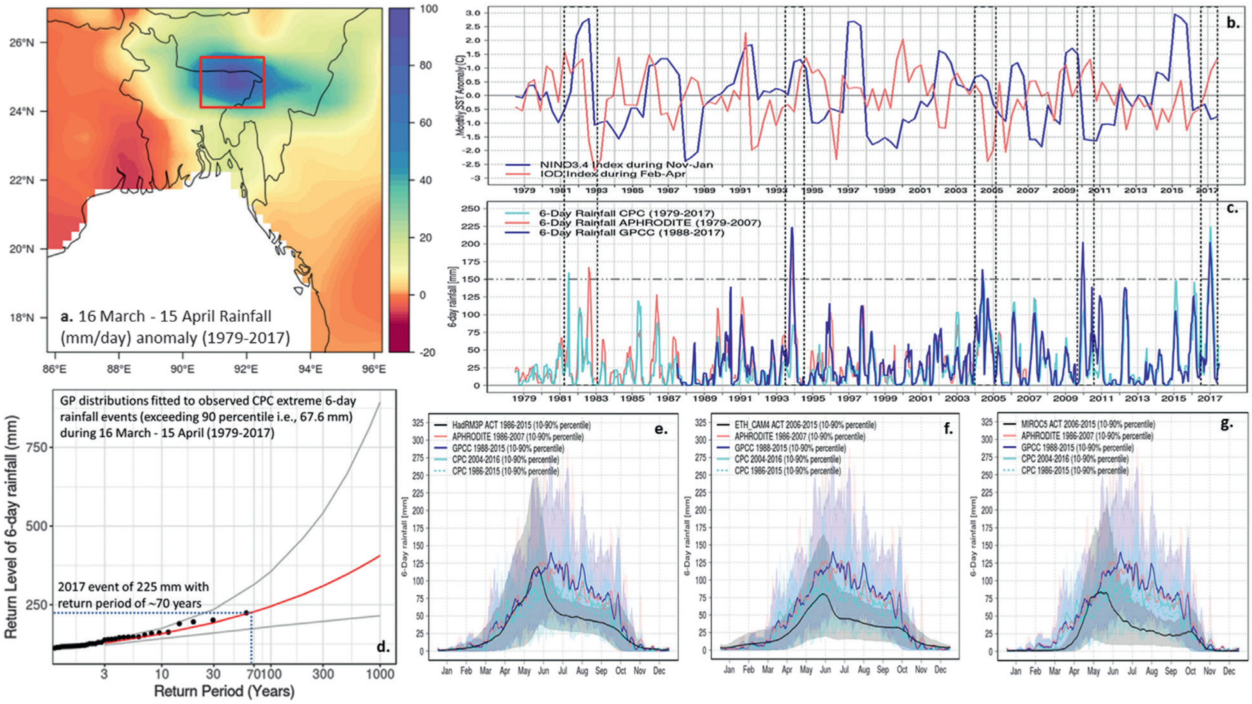

Fig. 1. (a) Spatial distribution of CPC rainfall (mm day^{-1}) over Bangladesh during 16 March–15 April 2017 relative to climatology (1979–2017). The red box indicates the study area of NEB. (b) Niño-3.4 (November–January) and IOD (February–April) indices during 1979–2017. The horizontal dashed black line in (c) indicates the threshold value for heaviest rainfall events. The vertical dashed black rectangles in (b) and (c) indicate the association between the heaviest rainfall events and IOD (Niño-3.4). (d) Return level plot of GP distribution fitted to CPC observed extreme 6-day rainfall events exceeding a 90th percentile threshold. (e)–(g) Annual cycles of 6-day rainfall over NEB as in models and observations (HadRM3P, ETH_CAM4 and MIROC5, respectively), with CPC (1979–2017 and 2004–16), GPCC (1988–2017), and APHRODITE (1979–2007).

(Yatagai et al. 2012), CPC global 0.5° analysis of daily rain gauge measurements covering 1979–2017 (Chen et al. 2008), and Global Rainfall Climatology Centre (GPCC) daily rainfall data covering 1988–2017 (Schamm et al. 2015). The higher-resolution (50 km) weather@home HadRM3P RCM is nested in the global atmosphere-only HadAM3P model [an atmospheric general circulation model (AGCM)] and is driven by prescribed SSTs and sea ice concentration (SIC) (Massey et al. 2015; Guillod et al. 2017) and radiative forcing. Following Schaller et al. (2016), we use 75,000 (30 × 2500) simulations for "Actual March 2017" under factual conditions with observed 2017 GHG concentrations, OSTIA SSTs, and SIC (Donlon et al. 2012) and 15,7500 (30 × 5250) simulations for "Natural March 2017" under conditions that might have been in a counterfactual world without past GHG emissions and other pollutants. We also use 2,160,000 (360 × 30 × 200) simulations for each of the Actual, Natural, and GHG-only climatology over the 30 years (1986–2015) of reference period. Here the GHG-only scenario has current levels of GHGs but the anthropogenic aerosols are set to pre-industrial levels. In addition, we use smaller ensembles from two GCMs, with 1500 (30 × 50) simulations from MIROC5 and 15,000 (30 × 500) simulations from ETH_CAM4 representing Actual and Natural March during a 10-yr (2006–15) period [see Mitchell et al. (2017) for more details]. All model and observation data are regridded using bilinear interpolation method and then area-averaged rainfall statistics over NEB are analyzed. We use the Niño-3.4 index (Rayner et al. 2003) to determine the lagged correlation with March rainfall over NEB, and with the IOD index (Huang et al. 2017).

We quantified the change in the occurrence probability of rainfall event, the risk ratio (RR), as RR = P_f/P_{cf}, where the probability of the event in the factual climate is denoted by P_f and the probability of the same event in a counterfactual climate without anthropogenic climate change is denoted by P_{cf} (NAS 2016). An exception to this is the GHG-only scenario, where RR is calculated using P_{cf} = actual climate instead of natural climate.

As far as the HadRM3P's performance with regard to APHRODITE, GPCC, and CPC is concerned, the

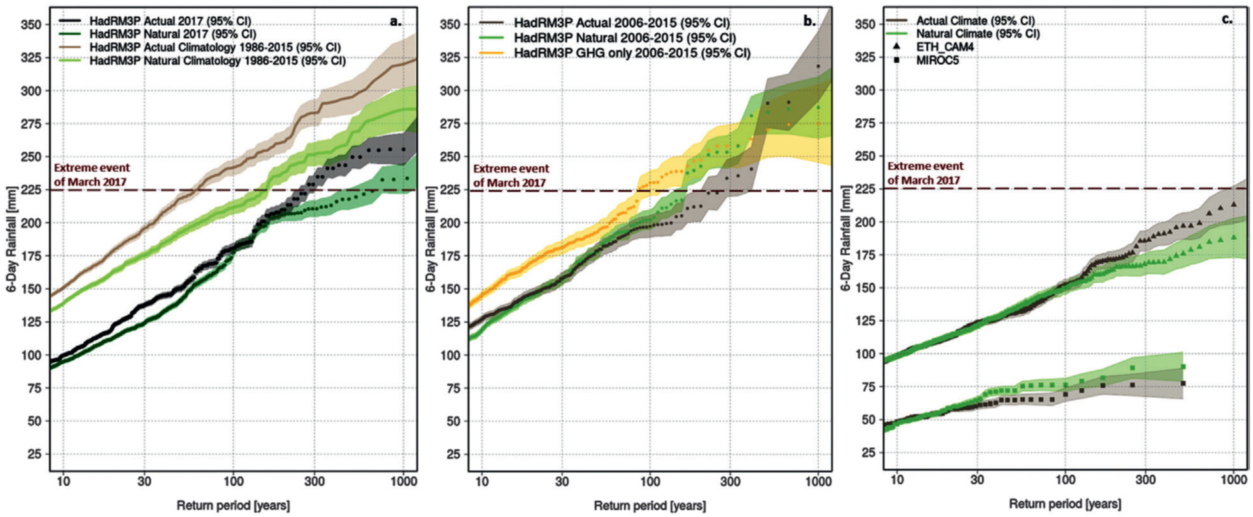

Fig. 2. Return periods for 6-day rainfall events in March over NEB showing (a) HadRM3P Actual 2017 (black) and Natural 2017 (dark green) vs Actual climatology 1986–2015 (gray) and Natural climatology 1986–2015 (light green) ensembles. (b) Actual climatology 2006–15 (gray), Natural climatology 2006–15 (light green), and GHG-only climatology 2006–15 (yellow). (c) Actual climatology 2006–15 (gray) and Natural climatology 2006–15 (light green) but as in MIROC5 (squares) and ETH_CAM4 (triangles) model ensembles. Each dot, triangle, or square represents one simulation of the HadRM3P, MIROC5, or ETH_CAM4 model, respectively, and the shaded polygon shows 95% confidence intervals. The horizontal dashed deep brown line in each panel indicates the extreme event of March 2017.

model reproduces the annual rainfall cycle with satisfactory agreement. However, monsoon rainfall is underestimated in HadRM3P by ~30% (Fig. 1e) with an early onset. We are using model data for March rather than mid-March to mid-April to remove this bias. MIROC5 is biased dry (Fig. 1g) in March (~50%), whereas ETH-CAM4 (Fig. 1f) is biased extremely dry (~40% in March and ~25%–50% throughout the monsoon season).

RESULTS AND DISCUSSION. Figure 2 illustrates how the return periods of March extreme 6-day rainfall events have changed from natural counterfactual climate to actual climate scenarios. The likelihood of extreme 6-day rainfall event under 2017 SST conditions in March has increased by ~20% (Fig. 2a) in HadRM3P compared to natural conditions. We find RR of ~2 (100% increase) for the 1986–2015 climatology period (Fig. 2a), but then unaltered risks for the shorter 2006–15 period (for events < 200 mm; Fig. 2b). This suggests that there are interesting nonlinear dynamic feedbacks at play, which depend on the state of the climate (i.e., ENSO or IOD variability). For March and the preceding winter (DJF 2016/17), very weak La Niña conditions were present (see Fig. ES2c in the online supplemental material). While not conclusive, HadRM3P results indicate that La Niña made drier conditions more likely over NEB (Fig. ES1c). Such feedback arises from global teleconnections, which can be detected in the upper-level zonal wind anomaly fields, in HadRM3P and reanalysis (not shown). In general, we find a moderate correlation ($r = 0.4$ to 0.6; no lag) between Niño-3.4 and NEB rainfall in March (Fig. ES2g). Regarding the interplay between ENSO and IOD itself, we argue that ENSO leads most IOD changes as notable particularly during strong El Niño events (Figs. 1b,c) because correlation between Niño-3.4 during November to January and IOD during February and March ($r = 0.467$; 4 months' lead time; $p = 0.0081$ at 95% confidence level) is significant. While positive IOD events tend to weaken the El Niño impact on the rainfall (e.g., Behera and Ratnam 2018), we obtain mixed results for the five heavy rainfall events (vertical dashed rectangles through Figs. 1b and 1c) exceeding the 150-mm threshold. Only two out of five events were associated with positive IOD and El Niño conditions. March 2017 is drier not only from an ENSO but also from an IOD point of view. Since March is in the beginning of the pre-monsoon season, small changes can cause drastically different outcomes. Matsumoto (1997) and Ashfaq et al. (2009) identified an early onset of the rainy days at NEB on 8 April and 21 May, respectively. We speculate that the current warming has shifted the pre-monsoon heavy rain's onset to even an earlier start. We notice a decreasing risk for the extreme rainfall event of March 2017 (225 mm) from Natural to Actual climate but then an increasing risk from natural to GHG-only climate conditions during 2006–15. This result demonstrates a considerable contribution of the anthropogenic aerosols for March 2006–15 (Fig. 2b); however, this is not the same for 1986–2015 (not shown). MIROC5 and ETH_CAM4 simulate much smaller changes in risk, with ETH_CAM4 even suggesting a drying trend, but none of these GCMs captured the observed extreme event of 2017 (Fig. 2c).

CONCLUSIONS. Based on the results from HadRM3P model only (for 1986–2015), we conclude that anthropogenic climate change doubled the likelihood of extreme pre-monsoon rainfall (~100% more likely) over NEB. Interestingly, the attribution signal in March is sensitive to the chosen climatology period. Natural ENSO and IOD variability influence interannual changes in rainfall risks, yet both indices made the 2017 rainfall event less likely. The anthropogenic aerosol cooling effect is noticeably observed during the recent decade (2006–15). How the interplay between the two competing forces of GHGs and the anthropogenic aerosols influences the risks of extreme rainfall events should be explored more. For the first time, this study presents attribution assessment for pre-monsoon extreme rainfall event for Bangladesh. Understanding the physical mechanisms behind such event and using a multimodel approach to incorporate associated uncertainties can be useful for further studies.

ACKNOWLEDGMENTS. We thank our colleagues at the Oxford e-Research Centre for their technical expertise, the Met Office Hadley Centre PRECIS team for their technical and scientific support for the development and application of weather@home, and all the volunteers who have donated their computing time to climateprediction.net and weather@home.

REFERENCES

Allen, M: 1999: Do-it-yourself climate prediction. *Nature*, **401**, 642, https://doi.org/10.1038/44266.

Ahmed, R., K. R. Rahaman, A. Kok, and Q. K. Hassan, 2017: Remote sensing-based quantification of the impact of flash flooding on the rice production: A case study over northeastern Bangladesh. *Sensors*, **17**, E2347, https://doi.org/10.3390/s17102347.

Ashfaq, M., Y. Shi, W.-W. Tung, R. J. Trapp, X. Gao, J. S. Pal, and N. S. Diffenbaugh, 2009: Suppression of South Asian summer monsoon precipitation in the 21st century. *Geophys. Res. Lett.*, **36**, L01704, https://doi.org/10.1029/2008GL036500.

Behera, S. K., and J. V. Ratnam, 2018: Quasi-asymmetric response of the Indian summer monsoon rainfall to opposite phases of the IOD. *Sci. Rep.*, **8**, 123, https://doi.org/10.1038/s41598-017-18396-6.

Black, M. T., and Coauthors, 2016: The weather@home regional climate modelling project for Australia and New Zealand. *Geosci. Model Dev.*, **9**, 3161–3176, https://doi.org/10.5194/gmd-9-3161-2016.

Chen, M., W. Shi, P. Xie, V. Silva, V. Kousky, R. Higgins, and J. Janowiak, 2008: Assessing objective techniques for gauge-based analyses of global daily precipitation. *J. Geophys. Res.*, **113**, D04110, https://doi.org/10.1029/2007JD009132.

Donlon, C. J., M. Martin, J. Stark, J. Roberts-Jones, E. Fiedler, and W. Wimmer, 2012: The Operational Sea Surface Temperature and Sea Ice Analysis (OSTIA) system. *Remote Sens. Environ.*, **116**, 140–158, https://doi.org/10.1016/j.rse.2010.10.017.

FAO, 2017: Bangladesh: Severe floods in 2017 affected large numbers of people and caused damage to the agriculture sector. Food and Agriculture Organization of the United Nations, 6 pp., www.fao.org/3/a-i7876e.pdf.

Guillod, B. P., and Coauthors, 2017: weather@home 2: Validation of an improved global-regional climate modelling system. *Geosci. Model Dev.*, **10**, 1849–1872, https://doi.org/10.5194/gmd-10-1849-2017.

Hansen, J., R. Ruedy, M. Sato, and K. Lo, 2010: Global surface temperature change. *Rev. Geophys.*, **48**, RG4004, https://doi.org/10.1029/2010RG000345.

Huang, B., and Coauthors, 2017: Extended Reconstructed Sea Surface Temperature, version 5 (ERSSTv5): Upgrades, validations, and intercomparisons. *J. Climate*, **30**, 8179–8205, https://doi.org/10.1175/JCLI-D-16-0836.1.

IPCC, 2013: *Climate Change 2013: The Physical Science Basis*. T. F. Stocker et al., Eds., Cambridge University Press, 1535 pp.

Li, Z., and Coauthors, 2016: Aerosol and monsoon climate interactions over Asia. *Rev. Geophys.*, **54**, 866–929, https://doi.org/10.1002/2015RG000500.

Marthews, T. R., F. E. L. Otto, D. Mitchell, S. J. Dadson, and R. G. Jones, 2015: The 2014 drought in the horn of Africa: Attribution of meteorological drivers [in "Explaining Extreme Events of 2014 from a Climate Perspective"]. *Bull. Amer. Meteor. Soc.*, **96**, S83–S88, https://doi.org/10.1175/BAMS-D-15-00115.1.

Massey, N., and Coauthors, 2015: weather@home—Development and validation of a very large ensemble modelling system for probabilistic event attribution. *Quart. J. Roy. Meteor. Soc.*, **141**, 1528–1545, https://doi.org10.1002/qj.2455.

Matsumoto, J., 1997: Seasonal transition of summer rainy season over Indochina and adjacent monsoon region. *Adv. Atmos. Sci.*, **14**, 231–245, https://doi.org/10.1007/s00376-997-0022-0.

Mitchell, D., K. and Coauthors, 2017: Half a degree additional warming, prognosis and projected impacts (HAPPI): Background and experimental design. *Geosci. Model Dev.*, **10**, 571–583, https://doi.org/10.5194/gmd-10-571-2017.

Murata, F., T. Terao, T. Hayashi, H. Asada, and J. Matsumoto, 2008: Relationship between atmospheric conditions at Dhaka, Bangladesh, and rainfall at Cherrapunjee, India. *Nat. Hazards*, **44**, 399–410, https://doi.org/10.1007/s11069-007-9125-2.

——, and Coauthors, 2011: Daytime thermodynamic and air flow structures over northeast Bangladesh during the pre-monsoon season: A case study on 25 April 2010. *J. Meteor. Soc. Japan*, **89A**, 167–179, https://doi.org/10.2151/jmsj.2011-A11.

NAS, 2016: *Attribution of Extreme Weather Events in the Context of Climate Change*. National Academies of Sciences, Engineering and Medicine, 186 pp.

Otto, F. E. L., 2017: Attribution of weather and climate events. *Annu. Rev. Environ. Resour.*, **42**, 627–646, https://doi.org/10.1146/annurev-environ-102016-060847.

——, R. James, and M. Allen, 2015: The science of attributing extreme weather events and its potential contribution to assessing loss and damage associated with climate change impacts. Environmental Change Institute, 4 pp., https://unfccc.int/files/adaptation/workstreams/loss_and_damage/application/pdf/attributingextremeevents.pdf.

Rayner, N. A., D. E. Parker, E. B. Horton, C. K. Folland, L. V. Alexander, D. P. Rowell, E. C. Kent, and A. Kaplan, 2003: Global analyses of sea surface temperature, sea ice, and night marine air temperature since the late nineteenth century. *J. Geophys. Res.*, **108**, 4407, https://doi.org/10.1029/2002JD002670.

Sanderson, M., and R. Ahmed, 1979: Pre-monsoon rainfall and its variability in Bangladesh: A trend surface analysis. *Hydrol. Sci. Bull.*, **24**, 277–287, https://doi.org/10.1080/02626667909491867.

Schaller, N., and Coauthors, 2016: Human influence on climate in the 2014 southern England winter floods and their impacts. *Nat. Climate Change*, **6**, 627–634, https://doi.org/10.1038/nclimate2927.

Schamm, K., M., Ziese, K. Raykova, A. Becker, P. Finger, A. Meyer-Christoffer, and U. Schneider, 2015: GPCC full data daily version 1.0 at 1.0°: Daily land-surface precipitation from rain-gauges built on GTS-based and historic data, accessed 10 Dec 2017, https://doi.org/10.5676/DWD_GPCC/FD_D_V1_100.

Shahid, S., 2010: Rainfall variability and the trends of wet and dry periods in Bangladesh. *Int. J. Climatol.*, **30**, 2299–2313, https://doi.org/10.1002/joc.2053.

Yatagai, A., K. Kenji, A. Osamu, H. Atsushi, Y. Natsuko, and K. Akio, 2012: APHRODITE: Constructing a long-term daily gridded precipitation dataset for Asia based on a dense network of rain gauges. *Bull. Amer. Meteor. Soc.*, **93**, 1401–1415, https://doi.org/10.1175/BAMS-D-11-00122.1.